

A NUMERICAL STUDY ON THE WEAK GALERKIN METHOD FOR THE HELMHOLTZ EQUATION WITH LARGE WAVE NUMBERS

LIN MU*, JUNPING WANG[†], XIU YE[‡], AND SHAN ZHAO[§]

Abstract. Weak Galerkin (WG) refers to general finite element methods for partial differential equations in which differential operators are approximated by weak forms through the usual integration by parts. In particular, WG methods allow the use of discontinuous finite element functions in the algorithm design. One of such examples was recently introduced in [54] for solving second order elliptic problems. The goal of this paper is to apply the WG method of [54] to the Helmholtz equation with high wave numbers. Several test scenarios are designed for a numerical investigation on the accuracy, convergence, and robustness of the WG method in both inhomogeneous and homogeneous media over convex and non-convex domains. Our numerical experiments indicate that weak Galerkin is a finite element technique that is easy to implement, and provides very accurate and robust numerical solutions for the Helmholtz problem with high wave numbers.

Key words. Galerkin finite element methods, discrete gradient, the Helmholtz equation, weak Galerkin

AMS subject classifications. Primary, 65N15, 65N30, 76D07; Secondary, 35B45, 35J50

1. Introduction. In this paper, we explore the use of a weak Galerkin (WG) finite element method for solving the nonhomogeneous Helmholtz equation with high wave numbers

$$(1.1) \quad -\nabla \cdot (d\nabla u) - k^2 u = f,$$

where k is the wave number, f represents a harmonic source, and $d = d(x, y)$ is a spatial function describing the dielectric properties of the medium. The Helmholtz equation (1.1) governs many macroscopic wave phenomena in the frequency domain including wave propagation, guiding, radiation and scattering, where the time-harmonic behavior can be assumed. The numerical solution to the Helmholtz equation plays a vital role in a wide range of applications in electromagnetics, optics, and acoustics, such as antenna analysis and synthesis, radar cross section calculation, simulation of ground or surface penetrating radar, design of optoelectronic devices, acoustic noise control, and seismic wave propagation. However, it remains a challenge to design robust and efficient numerical algorithms for the Helmholtz equation, especially when high wave numbers or highly oscillatory solutions are involved [58].

Physically, the Helmholtz problem is usually defined on an unbounded exterior domain with the so-called Sommerfeld radiation condition holding at infinity [38, 53]

$$(1.2) \quad \frac{\partial u}{\partial r} - iku = o\left(r^{\frac{1-m}{2}}\right), \quad \text{as } r \rightarrow \infty, \quad m = 2, 3.$$

*Department of Applied Science, University of Arkansas at Little Rock, Little Rock, AR 72204 (lxmu@ualr.edu).

[†]Division of Mathematical Sciences, National Science Foundation, Arlington, VA 22230 (jwang@nsf.gov). The research of Wang was supported by the NSF IR/D program, while working at the Foundation. However, any opinion, finding, and conclusions or recommendations expressed in this material are those of the author and do not necessarily reflect the views of the National Science Foundation.

[‡]Department of Mathematics and Statistics, University of Arkansas at Little Rock, Little Rock, AR 72204 (xye@ualr.edu). This research of Ye was supported in part by National Science Foundation Grant DMS-1115097.

[§]Department of Mathematics, University of Alabama, Tuscaloosa, AL 35487 (szhao@bama.ua.edu). The research of Zhao was supported in part by National Science Foundation Grant DMS-1016579.

where $i = \sqrt{-1}$ is the imaginary unit and r is the radial direction. Here we have assumed that $d = 1$ in far field. In computational electromagnetics, the exterior domain problems are often solved numerically by introducing a bounded domain Ω with an artificial boundary $\partial\Omega$ and imposing certain boundary conditions on $\partial\Omega$ so that nonphysical reflections from the boundary can be eliminated or minimized. For the Helmholtz exterior problems, the non-reflecting condition is commonly chosen as a Dirichlet-to-Neumann (DtN) mapping, which relates the wave solution to its derivatives on $\partial\Omega$ [38, 53]

$$(1.3) \quad d\nabla u \cdot \mathbf{n} - T(u) = g, \quad \text{on } \partial\Omega,$$

where \mathbf{n} denotes the outward normal direction of $\partial\Omega$, T is a DtN integral operator, and g is a given data function. For sufficiently large Ω , the nonlocal boundary condition (1.3) can be approximated by a Robin boundary condition [38, 53]

$$(1.4) \quad d\nabla u \cdot \mathbf{n} - ik u = g, \quad \text{on } \partial\Omega,$$

which is essentially a first order absorbing boundary condition.

In the present paper, we consider the following prototype Helmholtz problem

$$(1.5) \quad -\nabla \cdot (d\nabla u) - k^2 u = f \quad \text{in } \Omega,$$

$$(1.6) \quad d\nabla u \cdot \mathbf{n} - ik u = g \quad \text{on } \partial\Omega.$$

Finite element methods for such Helmholtz problems can be classified as two categories. The first category consists of methods that use continuous functions to approximate the solution u and the other refers to methods with discontinuous approximation functions.

Continuous Galerkin (CG) finite element methods employ continuous piecewise polynomials to approximate the true solution of (1.5)-(1.6) and lead to a simple formulation: find $u_h \in V_h \subset H^1(\Omega)$ satisfying

$$(1.7) \quad (d\nabla u_h, \nabla v_h) - k^2(u_h, v_h) + ik(u_h, v_h)_{\partial\Omega} = (f, v_h) + (g, v_h)_{\partial\Omega}$$

for all $v_h \in V_h$, where V_h is an properly defined finite element space consisting of continuous piecewise polynomials.

Discontinuous Galerkin (DG) finite element methods for the Helmholtz equation with $d = 1$ (e.g. [33]) seek $u_h \in V_h \subset L^2(\Omega)$ satisfying

$$(1.8) \quad \begin{aligned} & \sum_T (\nabla u_h, \nabla v_h)_T - \sum_e ((\{\nabla u_h\}, [v_h])_e + \sigma(\{\nabla v_h\}, [u_h])_e) - k^2(u_h, v_h) \\ & \quad + ik(u_h, v_h)_{\partial\Omega} + i \left(\sum_e \alpha_1 h_e^{-1} ([u_h], [v_h])_e + \sum_e \alpha_2 h_e \left(\left[\frac{\partial u_h}{\partial \mathbf{n}} \right], \left[\frac{\partial v_h}{\partial \mathbf{n}} \right] \right)_e \right. \\ & \quad \left. + \sum_e \alpha_3 h_e^{-1} \left(\left[\frac{\partial u_h}{\partial \mathbf{t}} \right], \left[\frac{\partial v_h}{\partial \mathbf{t}} \right] \right)_e \right) = (f, v_h) + (g, v_h)_{\partial\Omega}, \end{aligned}$$

for all $v_h \in V_h$, where $\alpha_i, i=1,2,3$ are penalty parameters and V_h is a space of discontinuous piecewise polynomials.

The continuous Galerkin finite element formulation (1.7) is natural and easy to implement. However, the errors of continuous Galerkin finite element solutions deteriorate rapidly when k becomes large. On the other hand, the formulation of DG

methods (1.8) is complex, and the stability and accuracy of DG methods heavily depend on the selection of penalty parameters (a good determination for the parameter values has been an issue for DG methods).

The objective of the present paper is to introduce a weak Galerkin (WG) finite element method for solving the Helmholtz problem with high wave numbers and to investigate the robustness and effectiveness of such WG method through many carefully designed numerical experiments. The weak Galerkin finite element formulation was first developed in [54] for solving the second order elliptic equations. Through rigorous error analysis, optimal order of convergence of the WG solution in both discrete H^1 norm and L^2 norm is established under minimum regularity assumptions in [54]. Nevertheless, no experimental results have been reported in [54].

Generally speaking, like the DG method, the WG finite element method allows one to use discontinuous functions in the finite element procedure. The main idea behind weak Galerkin methods lies in the approximation of differential operators by weak forms for discontinuous finite element functions defined on a partition of the domain. For example, for the gradient operator, one may introduce a weak gradient operator ∇_d over discontinuous functions $v_h = \{v_0, v_b\}$, where v_0 is defined in the interior of the element and v_b is defined on the boundary of the element. The weak gradient operator will then be employed to form a weak Galerkin finite element formulation for (1.5)-(1.6): find $u_h \in V_h$ such that for all $v_h \in V_h$ we have

$$(1.9) \quad (d\nabla_d u_h, \nabla_d v_h) - k^2(u_0, v_0) + ik(u_b, v_b)_{\partial\Omega} = (f, v_0) + (g, v_b)_{\partial\Omega}.$$

The discrete gradient $\nabla_d v$ in (1.9) is a variable locally calculated on each element. The weak Galerkin methods have many nice features. First, the formulation of WG method is simple, easy to implement, and involves no penalty parameters for users to select. The weak Galerkin is equipped with elements of polynomials of any degree $k \geq 0$. Secondly, the weak Galerkin method conserves mass with a well defined numerical flux. In some sense, weak Galerkin finite element methods enjoy both the simplicity of CG method and the flexibility of DG method.

In the present numerical investigation, we are particularly interested in the performance of the WG method for solving the Helmholtz equation with high wave numbers. In general, the numerical performance of any finite element solution to the Helmholtz equation depends significantly on the wave number k . When k is very large – representing a highly oscillatory wave, the mesh size h has to be sufficiently small for the scheme to resolve the oscillations. To keep a fixed grid resolution, a natural rule is to choose kh to be a constant in the mesh refinement, as the wave number k increases [41, 12]. However, it is known [41, 42, 8, 9] that, even under such a mesh refinement, the errors of continuous Galerkin finite element solutions deteriorate rapidly when k becomes larger. This non-robust behavior with respect to k is known as the “pollution effect” [41, 42, 8, 9]. Usually, under the small magnitude assumption of kh , the relative error of a p th order finite element solution in the H^1 -semi-norm consists of two parts [41, 42], i.e., an error term of the best approximation behavior like $O(k^p h^p)$ and a pollution error term behavior like $O(k^{2p+1} h^{2p})$. The error of best approximation is essentially due to the interpolation error on a discretized grid and is of bounded magnitude if $kh = \text{constant}$. Nevertheless, the pollution error term dominates when k is large and is responsible for the non-robustness behavior in the finite element solutions to the Helmholtz equation.

To the end of eliminating or substantially reducing the pollution errors, various numerical approaches have been developed in the literature for solving the Helmholtz

equation. For the continuous and least-squares finite element methods, a popular strategy [8, 9, 45, 10, 46] to reduce the pollution error is to include some analytical knowledge of the problem, such as characteristics of asymptotic or exact solution, in the finite element space. The resulting local basis functions of non-polynomial shape yield improved performance [8, 9, 45, 10, 46]. Similarly, analytical information is incorporated in the basis functions of the boundary element methods to address the high frequency problems [36, 44, 23]. Based on the geometrical optics and geometrical theory of diffraction, asymptotic solutions of the Helmholtz equation that represent important wave propagation directions are coupled with high frequency oscillations to build boundary element approximation spaces. Consequently, the number of degrees of freedom of such boundary element methods virtually does not depend on the wave number k for the Helmholtz equation [36, 44, 23]. In [22], plane wave solutions traveling in a large number of directions have also been employed as basis functions in the ultra weak variational formulation (UWVF) [21]. This allows the use of a coarse mesh when resolving high oscillatory wave solutions. The UWVF method can be regarded as an upwinding DG discretization for a first order system obtained through the introduction of an adjoint field. Based on such a viewpoint, error estimates of the UWVF on the entire domain have been recently presented in [19]. Multiple plane wave basis functions are also employed in a DG method using both low order elements [31] and high order elements [32]. The weak continuity of the solution at the element boundaries is enforced by introducing a Lagrange multiplier. Being more robust than classical variational approaches, this DG method can resolve high frequency short wave problems very well with a ratio of up to three wavelengths per element [31, 32].

Besides changing basis functions, there are other improvements that can be made in the DG framework to reduce the pollution error. By using piecewise linear polynomials as the basis functions, stable interior penalty DG methods have been developed in [33] through penalizing not only the jumps of the function values, but also the jumps of the normal and tangential derivatives across the element edges. Robust results against pollution effect can be achieved through a careful selection of penalty parameters [33]. Also targeting on enhancing stability, DG methods can be established by formulating the wave equation as a first-order system [6, 25]. The classical techniques, such as the enforcement of weak continuity via fluxes form, can be used in such DG solutions to the Helmholtz equation. The dispersive and dissipative behavior of selected DG schemes for both second order Helmholtz equation and the corresponding first order system have been examined in [2]. Hybridizable DG method is another efficient finite element method for the Helmholtz equation [29, 30]. By introducing new degree of freedoms on the boundary of elements, parametrization is conducted element by element so that the final linear system consists of unknowns only from the skeleton of the mesh. This greatly reduces the size of linear systems compared to the standard DG scheme. The error analysis [37] shows that the condition number of the condensed matrix of the hybridizable DG methods [29, 30] could be independent of the wave number.

The pollution effect can also be alleviated by controlling the numerical dispersion, i.e., the phase difference between the numerical and exact waves. This is because the pollution error is known to be directly related to the dispersion error [40, 1], while the best approximation error is non-dispersive. Thus, the reduction of the dispersive error is equivalent to the reduction of the pollution error. Consequently, high order methods, such as local spectral method [12], spectral Galerkin methods [52, 53], and spectral element methods [39, 3] are less vulnerable to the pollution effect, because

they produce negligible dispersive errors.

The rest of this paper is organized as follows. In Section 2, we will introduce a weak Galerkin finite element method for the Helmholtz equation by following the idea presented in [54]. In Section 3, we will present some error estimates for the WG method for the Helmholtz equation. Finally in Section 4, we shall present some numerical results obtained from the weak Galerkin method with various orders.

2. A Weak Galerkin Finite Element Method. Let \mathcal{T}_h be a partition of the domain Ω with mesh size h . Assume that the partition \mathcal{T}_h is shape regular so that the routine inverse inequality in the finite element analysis holds true (see [26]). Define $(v, w)_K = \int_K v w dx$ and $(v, w)_{\partial K} = \int_{\partial K} v w ds$.

For each triangle $T \in \mathcal{T}_h$, let T^0 and ∂T denote the interior and boundary of T respectively. Denote by $P_j(T^0)$ the set of polynomials in T^0 with degree no more than j , and $P_\ell(\partial T)$ the set of polynomials on each segment (edge or face) of ∂T with degree no more than ℓ . We emphasize that functions of $P_\ell(\partial T)$ are defined on each edge/face and there is no continuity required across different edges/faces. Define a global function $v = \{v_0, v_b\}$ where v_0 and v_b represent the values of v on T^0 and ∂T respectively for each $T \in \mathcal{T}_h$. Now we are ready to define a weak Galerkin finite element space as follows

$$(2.1) \quad V_h = \{v = \{v_0, v_b\} : \{v_0, v_b\}|_T \in P_j(T^0) \times P_\ell(\partial T), \forall T \in \mathcal{T}_h\}.$$

For each $v = \{v_0, v_b\} \in V_h$, we define the discrete gradient of v on each element T by the following equation:

$$(2.2) \quad \int_T \nabla_d v \cdot q dT = - \int_T v_0 \nabla \cdot q dT + \int_{\partial T} v_b q \cdot \mathbf{n} ds, \quad \forall q \in V_r(T),$$

where $V_r(T)$ is a subspace of the set of vector-valued polynomials of degree no more than r on T .

For the purpose of easy demonstration, we consider a special 2-D weak Galerkin element of V_h and $V_r(T)$ with $j = \ell = k \geq 0$ in (2.1) and $V_r(T) = RT_k(T)$. More weak Galerkin elements can be found in [54]. Here $RT_k(T)$ is the usual Raviart-Thomas element [47] of order k which has the form

$$RT_k(T) = P_k(T)^2 + \tilde{P}_k(T)\mathbf{x},$$

where $\tilde{P}_k(T)$ is the set of homogeneous polynomials of degree k and $\mathbf{x} = (x_1, x_2)$.

WEAK GALERKIN ALGORITHM 1. *A numerical approximation for (1.5)-(1.6) can be obtained by seeking $u_h = \{u_0, u_b\} \in V_h$ such that for all $v_h = \{v_0, v_b\} \in V_h$*

$$(2.3) \quad (d\nabla_d u_h, \nabla_d v_h) - k^2(u_0, v_0) + ik(u_b, v_b)_{\partial\Omega} = (f, v_0) + (g, v_b)_{\partial\Omega}.$$

In the following, we will use the lowest order weak Galerkin element ($k=0$) as an example to demonstrate how one might implement weak Galerkin finite element method for solving the Helmholtz problem (1.5)-(1.6). Let $N(T)$ and $N(e)$ denote the number of triangles and the number of edges associated with triangulation \mathcal{T}_h . Let \mathcal{E}_h denote the union of the boundaries of the triangles T of \mathcal{T}_h . Let ϕ_i be a function which takes value one in the interior of triangle T_i and zero everywhere else. Let ψ_j be a function that takes value one on edge e_j and zero everywhere else. The weak Galerkin finite element space V_h with $k = 0$ has the form

$$V_h = \text{span}\{\phi_1, \dots, \phi_{N(T)}, \psi_1, \dots, \psi_{N(e)}\}.$$

The methodology of implementing WG is the same as that for continuous Galerkin finite element method except that the standard gradient operator ∇ must be replaced by the discrete gradient operator ∇_d . The discrete gradient operator is an extension of the standard gradient operator for smooth functions to non-smooth functions. Therefore, the key step of implementing weak Galerkin method is to compute a **local** variable $\nabla_d v$ for $v = \{v_0, v_b\} \in V_h$ element by element. For the case $k = 0$, we have $\nabla_d v \in RT_0(T)$ on each element $T \in \mathcal{T}_h$ where

$$RT_0(T) = \begin{pmatrix} a + cx \\ b + cy \end{pmatrix} = \text{span}\{\theta_1, \theta_2, \theta_3\}.$$

For example, we can choose θ_i as follows

$$\theta_1 = \begin{pmatrix} 1 \\ 0 \end{pmatrix}, \theta_2 = \begin{pmatrix} 0 \\ 1 \end{pmatrix}, \theta_3 = \begin{pmatrix} x \\ y \end{pmatrix}.$$

Thus on each element $T \in \mathcal{T}_h$, $\nabla_d v = \sum_{j=1}^3 c_j \theta_j$. Using the definition of discrete gradient (2.2), we find c_j by solving the following linear system:

$$\begin{pmatrix} (\theta_1, \theta_1)_T & (\theta_2, \theta_1)_T & (\theta_3, \theta_1)_T \\ (\theta_1, \theta_2)_T & (\theta_2, \theta_2)_T & (\theta_3, \theta_2)_T \\ (\theta_1, \theta_3)_T & (\theta_2, \theta_3)_T & (\theta_3, \theta_3)_T \end{pmatrix} \begin{pmatrix} c_1 \\ c_2 \\ c_3 \end{pmatrix} = \begin{pmatrix} -(v_0, \nabla \cdot \theta_1)_T + (v_b, \theta_1 \cdot \mathbf{n})_{\partial T} \\ -(v_0, \nabla \cdot \theta_2)_T + (v_b, \theta_2 \cdot \mathbf{n})_{\partial T} \\ -(v_0, \nabla \cdot \theta_3)_T + (v_b, \theta_3 \cdot \mathbf{n})_{\partial T} \end{pmatrix}.$$

The inverse of the above coefficient matrix can be obtained explicitly or numerically through a local matrix solver. Once $\nabla_d \phi_i$ and $\nabla_d \psi_j$ are computed, the rest of steps are the same as those for the classical finite element method.

3. Error Estimates. Denote by $Q_h u = \{Q_0 u, Q_b u\}$ the L^2 projection onto $P_j(T^0) \times P_j(\partial T)$. In other words, on each element T , the function $Q_0 u$ is defined as the L^2 projection of u in $P_j(T)$ and on ∂T , $Q_b u$ is the L^2 projection in $P_j(\partial T)$.

Consider the following Helmholtz problem:

$$(3.1) \quad -\nabla \cdot (d \nabla u) - k^2 u = f \quad \text{in } \Omega,$$

$$(3.2) \quad u = g \quad \text{on } \partial \Omega.$$

For weak Galerkin finite element space V_h defined in (2.1), we define V_h^0 a subspace of V_h with vanishing boundary values on $\partial \Omega$; i.e.,

$$V_h^0 := \{v = \{v_0, v_b\} \in V_h, v_b|_{\partial T \cap \partial \Omega} = 0, \forall T \in \mathcal{T}_h\}.$$

The weak Galerkin finite element method for the Helmholtz problem (3.1)-(3.2) is stated as follows.

WEAK GALERKIN ALGORITHM 2. *A numerical approximation for (3.1) and (3.2) can be obtained by seeking $u_h = \{u_0, u_b\} \in V_h$ satisfying $u_b = Q_b g$ on $\partial \Omega$ and the following equation:*

$$(3.3) \quad (d \nabla_d u_h, \nabla_d v) - k^2 (u_0, v_0) = (f, v_0), \quad \forall v = \{v_0, v_b\} \in V_h^0,$$

For a sufficiently small mesh size h , the following error estimate holds true. A proof of this error estimate can be found in [54].

THEOREM 3.1. *Let $u \in H^1(\Omega)$ be the solution (3.1) and (3.2), and u_h be a weak Galerkin approximation of u arising from (3.3). Assume that the exact solution u is*

sufficiently smooth such that $u \in H^{m+1}(\Omega)$ with $0 \leq m \leq k+1$. Then, there exists a constant C such that

$$(3.4) \quad \|\nabla_d(u_h - Q_h u)\| \leq C(h^m \|u\|_{m+1} + h^{1+s} \|f - Q_0 f\|)$$

$$(3.5) \quad \|u_h - Q_h u\| \leq C(h^{m+s} \|u\|_{m+1} + h^{1+s} \|f - Q_0 f\|),$$

provided that the dual problem of (3.1)-(3.2) has the $H^{m+s}(\Omega)$ regularity with $s \in (0, 1]$.

4. Numerical Experiments. In this section, we examine the WG method by testing its accuracy, convergence, and robustness for solving two dimensional Helmholtz equations. The pollution effect due to large wave numbers will be particularly investigated and tested numerically. For convergence tests, both piecewise constant and piecewise linear finite elements will be considered. To demonstrate WG's robustness, the Helmholtz equation in both homogeneous and inhomogeneous media will be solved on convex and non-convex computational domains. For simplicity, a structured triangular mesh is employed in all cases. The mesh generation and all computations are conducted in the MATLAB environment.

Two types of relative errors are measured in our numerical experiments. The first one is the relative L^2 error and the second is the relative H^1 error. The relative L^2 error is defined by

$$\frac{\|u_h - Q_h u\|}{\|Q_h u\|},$$

where u_h is the WG approximation to the solution u , and $Q_h u = \{Q_0 u, Q_b u\}$ is the L^2 projection onto $P_j(T^0) \times P_j(\partial T)$. In other words, on each element T , the function $Q_0 u$ is defined as the L^2 projection of u in $P_j(T)$ and on ∂T , $Q_b u$ is the L^2 projection in $P_j(\partial T)$. The relative H^1 error is defined in terms of the discrete gradient

$$\frac{\|\nabla_d(u_h - Q_h u)\|}{\|\nabla_d Q_h u\|}.$$

However, in the present study, the H^1 -semi-norm will be calculated as

$$\|u_h - Q_h u\|^2 = h_e^{-1} \langle u_0 - u_b - (Q_0 u - Q_b u), u_0 - u_b - (Q_0 u - Q_b u) \rangle_e$$

for the lowest order finite element (i.e., piecewise constants). For piecewise linear elements, we use the original definition of ∇_d to compute the H^1 -semi-norm $\|\nabla_d(u_h - Q_h u)\|$.

4.1. A convex Helmholtz problem. We first consider a homogeneous Helmholtz equation defined on a convex hexagon domain, which has been studied in [33]. The domain Ω is the unit regular hexagon domain centered at the origin $(0, 0)$, see Fig. 4.1 (left). Here we set $d = 1$ and $f = \sin(kr)/r$ in (1.5), where $r = \sqrt{x^2 + y^2}$. The boundary data g in the Robin boundary condition (1.6) is chosen so that the exact solution is given by

$$(4.1) \quad u = \frac{\cos(kr)}{k} - \frac{\cos k + i \sin k}{k(J_0(k) + iJ_1(k))} J_0(kr)$$

where $J_\xi(z)$ are Bessel functions of the first kind. Let \mathcal{T}_h denote the regular triangulation that consists of $6N^2$ triangles of size $h = 1/N$, as shown in Fig. 4.1 (left) for $T_{\frac{1}{8}}$.

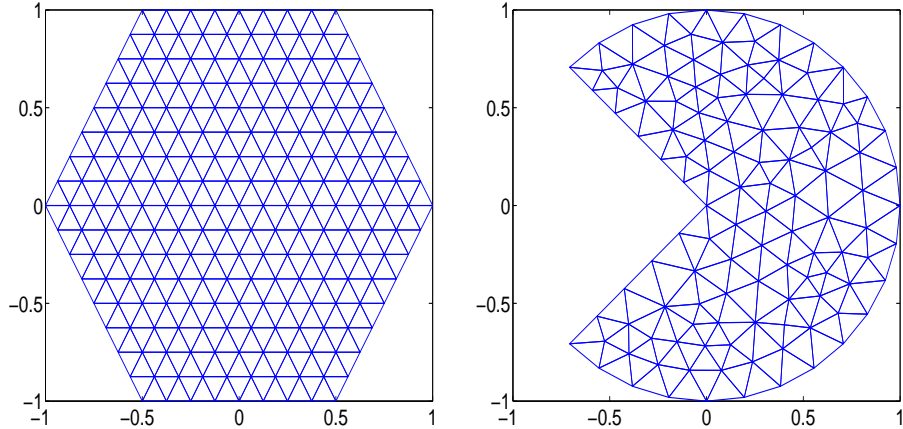


FIG. 4.1. Geometry of testing domains and sample meshes. Left: a convex hexagon domain; Right: a non-convex imperfect circular domain.

TABLE 4.1

Convergence of piecewise constant WG for the Helmholtz equation on a convex domain with wave number $k = 1$.

h	relative H^1		relative L^2	
	error	order	error	order
5.00e-01	2.49e-02		4.17e-03	
2.50e-01	1.11e-02	1.16	1.05e-03	1.99
1.25e-01	5.38e-03	1.05	2.63e-04	2.00
6.25e-02	2.67e-03	1.01	6.58e-05	2.00
3.13e-02	1.33e-03	1.00	1.64e-05	2.00
1.56e-02	6.65e-04	1.00	4.11e-06	2.00

TABLE 4.2

Convergence of piecewise linear WG for the Helmholtz equation on a convex domain with wave number $k = 5$.

h	relative H^1		relative L^2	
	error	order	error	order
2.50e-01	9.48e-03		2.58e-04	
1.25e-01	2.31e-03	2.04	3.46e-05	2.90
6.25e-02	5.74e-04	2.01	4.47e-06	2.95
3.13e-02	1.43e-04	2.00	5.64e-07	2.99
1.56e-02	3.58e-05	2.00	7.06e-08	3.00
7.81e-03	8.96e-06	2.00	8.79e-09	3.01

Table 4.1 illustrates the performance of the WG method with piecewise constant elements for the Helmholtz equation with wave number $k = 1$. Uniform triangular partitions were used in the computation through successive mesh refinements. The relative errors in L^2 norm and H^1 semi-norm can be seen in Table 4.1. The Table also includes numerical estimates for the rate of convergence in each metric. It can be seen that the order of convergence in the relative H^1 semi-norm and relative L^2 norm are, respectively, one and two for piecewise constant elements.

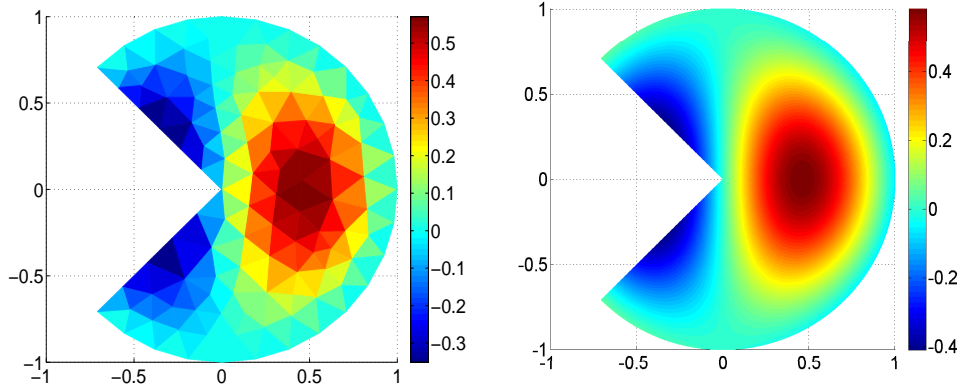


FIG. 4.2. WG solutions for the non-convex Helmholtz problem with $k = 4$ and $\xi = 1$. Left: Mesh level 1; Right: Mesh level 6.

High order of convergence can be achieved by using corresponding high order finite elements in the present WG framework. To demonstrate this phenomena, we consider the same Helmholtz problem with a slightly larger wave number $k = 5$. The WG with piecewise linear functions was employed in the numerical approximation. The computational results are reported in Table 4.2. It is clear that the numerical experiment validates the theoretical estimates. More precisely, the rates of convergence in the relative H^1 semi-norm and relative L^2 norm are given by two and three, respectively.

4.2. A non-convex Helmholtz problem. We next explore the use of the WG method for solving a Helmholtz problem defined on a non-convex domain, see Fig. 4.1 (right). The medium is still assumed to be homogeneous, i.e., $d = 1$ in (1.5). We are particularly interested in the performance of the WG method for dealing with the possible field singularity at the origin. For simplicity, only the piecewise constant RT_0 elements are tested for the present problem. Following [37], we take $f = 0$ in (1.5) and the boundary condition is simply taken as a Dirichlet one: $u = g$ on $\partial\Omega$. Here g is prescribed according to the exact solution [37]

$$(4.2) \quad u = J_\xi(k\sqrt{x^2 + y^2}) \cos(\xi \arctan(y/x)).$$

In the present study, the wave number was chosen as $k = 4$ and three values for the parameter ξ are considered; i.e., $\xi = 1$, $\xi = 3/2$ and $\xi = 2/3$. The same triangular mesh is used in the WG method for all three cases. In particular, an initial mesh is first generated by using MATLAB with default settings, see Fig. 4.1 (right). Next, the mesh is refined uniformly for five times. The WG solutions on mesh level 1 and mesh level 6 are shown in Fig. 4.2, Fig. 4.3, and Fig. 4.4, respectively, for $\xi = 1$, $\xi = 3/2$, and $\xi = 2/3$. Since the numerical errors are quite small for the WG approximation corresponding to mesh level 6, the field modes generated by the densest mesh are visually indistinguishable from the analytical ones. In other words, the results shown in the right charts of Fig. 4.2, Fig. 4.3, and Fig. 4.4 can be regarded as analytical results. It can be seen that in all three cases, the WG solutions already agree with the analytical ones at the coarsest level. Moreover, based on the coarsest mesh, the constant function values can be clearly seen in each triangle, due to the use of piecewise constant RT_0 elements. Nevertheless, after the initial mesh is refined for

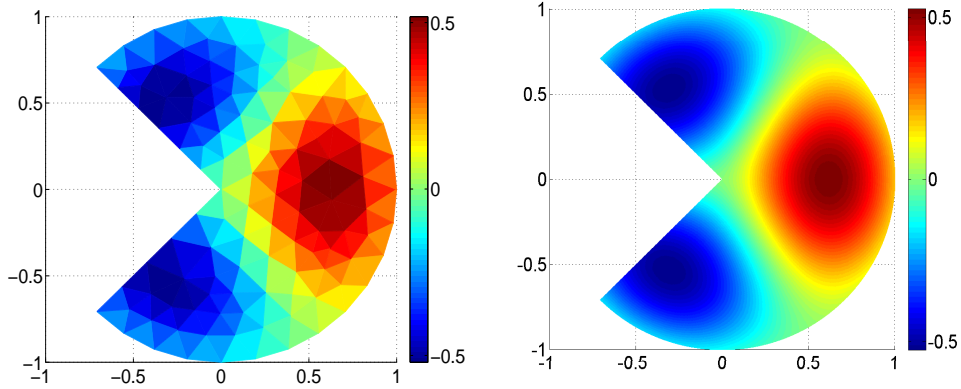


FIG. 4.3. WG solutions for the non-convex Helmholtz problem with $k = 4$ and $\xi = 3/2$. Left: Mesh level 1; Right: Mesh level 6.

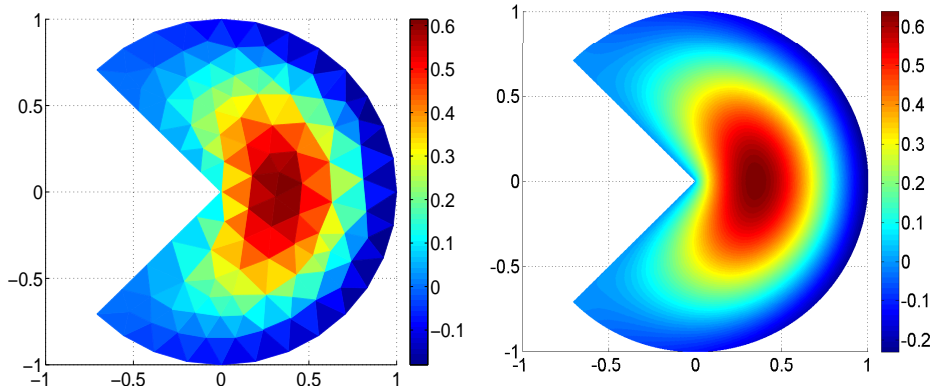


FIG. 4.4. WG solutions for the non-convex Helmholtz problem with $k = 4$ and $\xi = 2/3$. Left: Mesh level 1; Right: Mesh level 6.

TABLE 4.3

Numerical convergence test for the non-convex Helmholtz problem with $k = 4$ and $\xi = 1$.

h	relative H^1		relative L^2	
	error	order	error	order
2.44e-01	5.64e-02		1.37e-02	
1.22e-01	2.83e-02	1.00	3.56e-03	1.95
6.10e-02	1.42e-02	0.99	8.98e-04	1.99
3.05e-02	7.14e-03	1.00	2.25e-04	2.00
1.53e-02	3.57e-03	1.00	5.63e-05	2.00
7.63e-03	1.79e-03	1.00	1.41e-05	2.00

five times, the numerical plots shown in the right charts are very smooth. A perfect symmetry with respect to the x -axis is clearly seen.

We next investigate the numerical convergence rates for WG. The numerical errors of the WG solutions for $\xi = 1$, $\xi = 3/2$ and $\xi = 2/3$ are listed, respectively, in Table 4.3, Table 4.4, and Table 4.5. It can be seen that for $\xi = 1$ and $\xi = 3/2$, the

TABLE 4.4

Numerical convergence test for the non-convex Helmholtz problem with $k = 4$ and $\xi = 3/2$.

h	relative H^1		relative L^2	
	error	order	error	order
2.44e-01	5.56e-02		1.12e-2	
1.22e-01	2.81e-02	0.98	3.02e-03	1.89
6.10e-02	1.42e-02	0.99	8.06e-04	1.91
3.05e-02	7.14e-03	0.99	2.12e-04	1.92
1.53e-02	3.58e-03	1.00	5.54e-05	1.94
7.63e-03	1.79e-03	1.00	1.44e-05	1.95

TABLE 4.5

Numerical convergence test for the non-convex Helmholtz problem with $k = 4$ and $\xi = 2/3$.

h	relative H^1		relative L^2	
	error	order	error	order
2.44e-01	1.07e-01		5.24e-02	
1.22e-01	5.74e-02	0.90	2.18e-02	1.27
6.10e-02	3.23e-02	0.83	9.01e-03	1.27
3.05e-02	1.89e-02	0.77	3.68e-03	1.29
1.53e-02	1.14e-02	0.73	1.49e-03	1.31
7.63e-03	6.99e-03	0.71	5.96e-04	1.32

numerical convergence rates in the relative H^1 and L^2 errors remain to be first and second order, while the convergence orders degrade for the non-smooth case $\xi = 2/3$. Mathematically, for both $\xi = 3/2$ and $\xi = 2/3$, the exact solutions (4.2) are known to be non-smooth across the negative x -axis if the domain was chosen to be the entire circle. However, the present domain excludes the negative x -axis. Thus, the source term f of the Helmholtz equation (1.5) can be simply defined as zero throughout Ω . Nevertheless, there still exists some singularities at the origin $(0, 0)$. In particular, it is remarked in [37] that the singularity lies in the derivatives of the exact solution at $(0, 0)$. Due to such singularities, the convergence rates of high order DG methods are also reduced for $\xi = 3/2$ and $\xi = 2/3$ [37]. In the present study, we further note that there exists a subtle difference between two cases $\xi = 3/2$ and $\xi = 2/3$ at the origin. To see this, we neglect the second $\cos(\cdot)$ term in the exact solution (4.2) and plot the Bessel function of the first kind $J_\xi(k|r|)$ along the radial direction r , see Fig. 4.5. It is observed that the Bessel function of the first kind is non-smooth for the case $\xi = 2/3$, while it looks smooth across the origin for the case $\xi = 3/2$. Thus, it seems that the first derivative of $J_{3/2}(k|r|)$ is still continuous along the radial direction. This perhaps explains why the present WG method does not experience any order reduction for the case $\xi = 3/2$. In [37], locally refined meshes were employed to resolve the singularity at the origin so that the convergence rate for the case $\xi = 2/3$ can be improved. We note that local refinements can also be adopted in the WG method for a better convergence rate. A study of WG with grid local refinement is left to interested parties for future research.

4.3. A Helmholtz problem with inhomogeneous media. We consider a Helmholtz problem with inhomogeneous media defined on a circular domain with radius R . Note that the spatial function $d(x, y)$ in the Helmholtz equation (1.5)

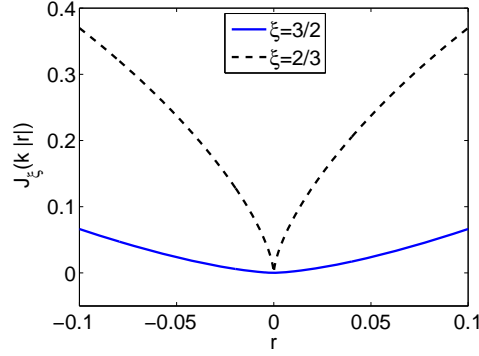


FIG. 4.5. The Bessel function of the first kind $J_\xi(k|r|)$ across the origin.

represents the dielectric properties of the underlying media. In particular, we have $d = \frac{1}{\epsilon}$ in the electromagnetic applications [56], where ϵ is the electric permittivity. In the present study, we construct a smooth varying dielectric profile:

$$(4.3) \quad d(r) = \frac{1}{\epsilon_1} S(r) + \frac{1}{\epsilon_2} (1 - S(r)),$$

where $r = \sqrt{x^2 + y^2}$, ϵ_1 and ϵ_2 are dielectric constants, and

$$(4.4) \quad S(r) = \begin{cases} 1 & \text{if } r < a, \\ -2 \left(\frac{b-r}{b-a} \right)^3 + 3 \left(\frac{b-r}{b-a} \right)^2 & \text{if } a \leq r \leq b, \\ 0 & \text{if } r > b, \end{cases}$$

with $a < b < R$. An example plot of $d(r)$ and $S(r)$ is shown in Fig. 4.6. In classical electromagnetic simulations, ϵ is usually taken as a piecewise constant, so that some sophisticated numerical treatments have to be conducted near the material interfaces to secure the overall accuracy [56]. Such a procedure can be bypassed if one considers a smeared dielectric profile, such as (4.3). We note that under the limit $b \rightarrow a$, a piecewise constant profile is recovered in (4.3). In general, the smeared profile (4.3) might be generated via numerical filtering, such as the so-called ϵ -smoothing technique [51] in computational electromagnetics. On the other hand, we note that the dielectric profile might be defined to be smooth in certain applications. For example, in studying the solute-solvent interactions of electrostatic analysis, some mathematical models [24, 57] have been proposed to treat the boundary between the protein and its surrounding aqueous environment to be a smoothly varying one. In fact, the definition of (4.3) is inspired by a similar model in that field [24].

In the present study, we choose the source of the Helmholtz equation (1.5) to be

$$(4.5) \quad f(r) = k^2[d(r) - 1]J_0(kr) + kd'(r)J_1(kr),$$

where

$$(4.6) \quad d'(r) = \left(\frac{1}{\epsilon_1} - \frac{1}{\epsilon_2} \right) S'(r)$$

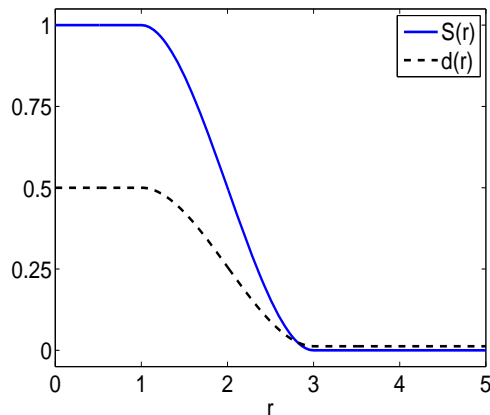


FIG. 4.6. An example plot of smooth dielectric profile $d(r)$ and $S(r)$ with $a = 1$, $b = 3$ and $R = 5$. The dielectric coefficients of protein and water are used, i.e., $\epsilon_1 = 2$ and $\epsilon_2 = 80$.

and

$$(4.7) \quad S'(r) = \begin{cases} 0 & \text{if } r < a, \\ 6 \left(\frac{b-r}{b-a} \right)^2 - 6 \left(\frac{b-r}{b-a} \right) & \text{if } a \leq r \leq b, \\ 0 & \text{if } b < r, \end{cases}$$

For simplicity, a Dirichlet boundary condition is imposed at $r = R$ with $u = g$. Here g is prescribed according to the exact solution

$$(4.8) \quad u = J_0(kr).$$

Our numerical investigation assumes the value of $a = 1$, $b = 3$ and $R = 5$. The wave number is set to be $k = 2$. The dielectric coefficients are chosen as $\epsilon_1 = 2$ and $\epsilon_2 = 80$, which represents the dielectric constant of protein and water [24, 57], respectively. The WG method with piecewise constant finite element functions is employed to solve the present problem with inhomogeneous media in Cartesian coordinate. Table 4.6 illustrates the computational errors and some numerical rate of convergence. It can be seen that the numerical convergence in the relative L^2 error is not uniform, while the relative H^1 error still converges uniformly in first order. This phenomena might be related to the non-uniformity and smallness of the media in part of the computational domain. Nevertheless, the averaged convergence rate in the relative L^2 norm is about 2.12. Overall, we are confident that the WG method is accurate and robust in solving the Helmholtz equations with inhomogeneous media.

4.4. Large wave numbers. We finally investigate the performance of the WG method for the Helmholtz equation with large wave numbers. The homogeneous Helmholtz problem studied in the Subsection 4.1 is employed again for this purpose. Also, the RT_0 and RT_1 elements are used to solve the homogeneous Helmholtz equation with the Robin boundary condition. Since this problem is defined on a structured hexagon domain, a uniform triangular mesh with a constant mesh size h throughout the domain is used. This enables us to precisely evaluate the impact of the mesh refinements. Following the literature works [12, 33], we will focus only on the relative H^1 semi-norm in the present study.

TABLE 4.6
Numerical convergence test of the Helmholtz equation with inhomogeneous media.

h	relative H^1		relative L^2	
	error	order	error	order
1.51e-00	2.20e-01		1.04e-00	
7.54e-01	1.24e-01	0.83	1.20e-01	3.11
3.77e-01	6.24e-02	0.99	1.81e-02	2.73
1.88e-01	3.13e-02	1.00	5.71e-03	1.67
9.42e-02	1.56e-02	1.00	2.14e-03	1.42
4.71e-02	7.82e-03	1.00	5.11e-04	2.06

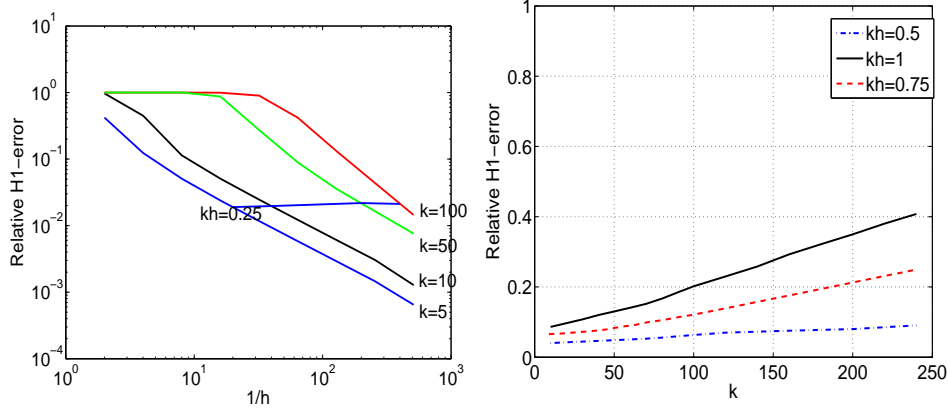


FIG. 4.7. Relative H^1 error of the WG solution. Left: with respect to $1/h$; Right: with respect to wave number k .

To study the non-robustness behavior with respect to the wave number k , i.e., the pollution effect, we solve the corresponding Helmholtz equation by using piecewise constant WG method with various mesh sizes for four wave numbers $k = 5$, $k = 10$, $k = 50$, and $k = 100$, see Fig. 4.7 (left) for the WG performance. From Fig. 4.7 (left), it can be seen that when h is smaller, the WG method immediately begins to converge for the cases $k = 5$ and $k = 10$. However, for large wave numbers $k = 50$ and $k = 100$, the relative error remains to be about 100%, until h becomes to be quite small or $1/h$ is large. This indicates the presence of the pollution effect. In the same figure, we also show the errors of different k values by fixing $kh = 0.25$. Surprisingly, we found that the relative H^1 error does not evidently increase as k becomes larger. The convergence line for $kh = 0.25$ looks almost flat, with a very little slope. We note that the present result of the WG method is as good as the one reported in [33] by using a penalized discontinuous Galerkin approach with optimized parameter values [33]. We emphasize that WG has advantage over the penalized DG in that no parameters are involved in the numerical scheme.

On the other hand, the good performance of the WG method for the case $kh = 0.25$ does not mean that the WG method could be free of pollution effect. In fact, it is known theoretically [9] that the pollution error cannot be eliminated completely in two- and higher-dimensional spaces for Galerkin finite element methods. In the right chart of Fig. 4.7, we examine the numerical errors by increasing k , under the constraint that kh is a constant. Huge wave numbers, up to $k = 240$, are tested.

It can be seen that when the constant changes from 0.5 to 0.75 and 1.0, the non-robustness behavior against k becomes more and more evident. However, the slopes of $kh=\text{constant}$ lines remain to be small and the increment pattern with respect to k is always monotonic. This suggests that the pollution error is well controlled in the WG solution.

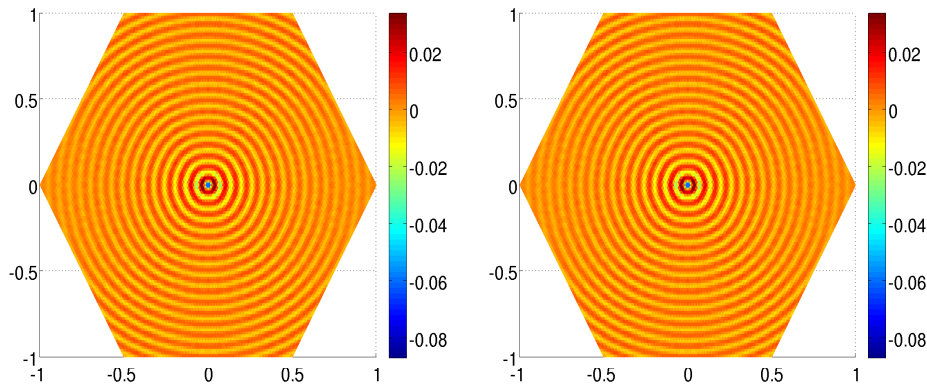


FIG. 4.8. *Exact solution (left) and piecewise constant WG approximation (right) for $k = 100$, and $h = 1/60$.*

In the rest of the paper, we shall present some numerical results for the WG method when applied to a challenging case of high wave numbers. In Fig. 4.8 and 4.10, the WG numerical solutions are plotted against the exact solution of the Helmholtz problem. Here we take a wave number $k = 100$ and mesh size $h = 1/60$ which is relatively a coarse mesh. With such a coarse mesh, the WG method can still capture the fast oscillation of the solution. However, the numerically predicted magnitude of the oscillation is slightly damped for waves away from the center when piecewise constant elements are employed in the WG method. Such damping can be seen in a trace plot along x -axis or $y = 0$. To see this, we consider an even worse case with $k = 100$ and $h = 1/50$. The result is shown in the first chart of Fig. 4.9. We note that the numerical solution is excellent around the center of the region, but it gets worse as one moves closer to the boundary. If we choose a smaller mesh size $h = 1/120$, the visual difference between the exact and WG solutions becomes very small, as illustrate in Fig. 4.9. If we further choose a mesh size $h = 1/200$, the exact solution and the WG approximation look very close to each other. This indicates an excellent convergence of the WG method when the mesh is refined. In addition to mesh refinement, one may also obtain a fast convergence by using high order elements in the WG method. Figure 4.11 illustrates a trace plot for the case of $k = 100$ and $h = 1/60$ when piecewise linear elements are employed in the WG method. It can be seen that the computational result with this relatively coarse mesh captures both the fast oscillation and the magnitude of the exact solution very well.

5. Concluding Remarks. The numerical experiments indicate that the WG method as introduced in [54] is a very promising numerical technique for solving the Helmholtz equations with large wave numbers. This finite element method is robust, efficient, and easy to implement. On the other hand, a theoretical investigation for the WG method should be conducted by taking into account some useful features of the Helmholtz equation when special test functions are used. It would also be valuable to

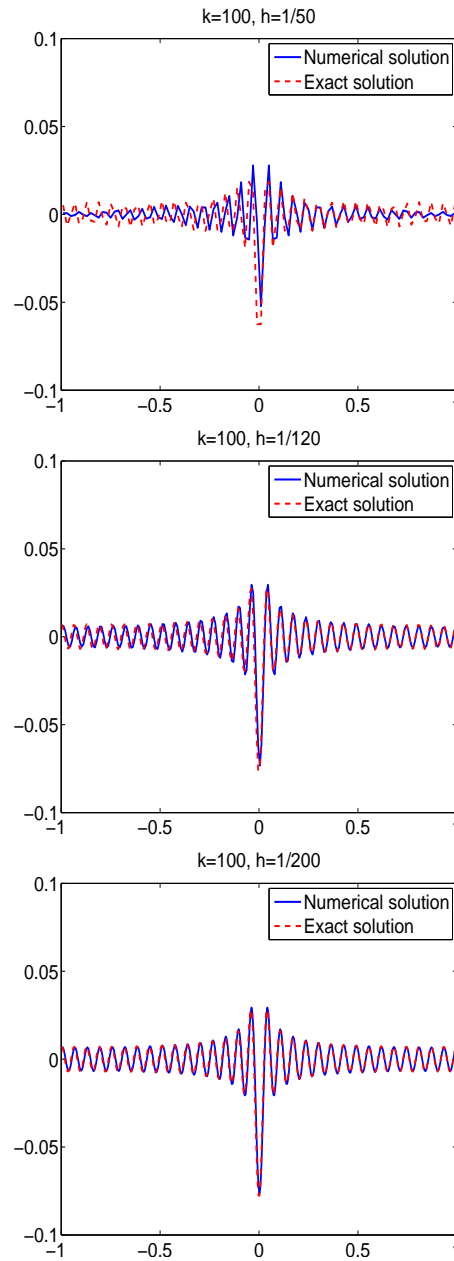


FIG. 4.9. The trace plot along x -axis or $y = 0$ form WG solution using piecewise constants.

test the performance of the WG method when high order finite elements are employed to the Helmholtz equations with large wave numbers in two and three dimensional spaces.

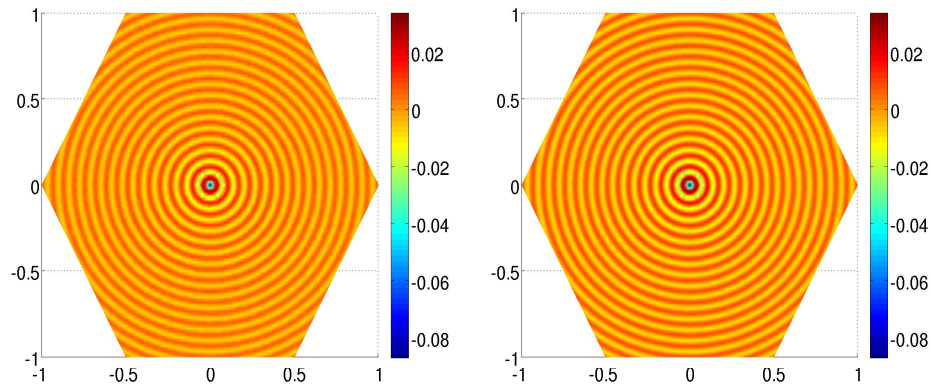


FIG. 4.10. *Exact solution (left) and piecewise linear WG approximation (right) for $k = 100$, and $h = 1/60$.*

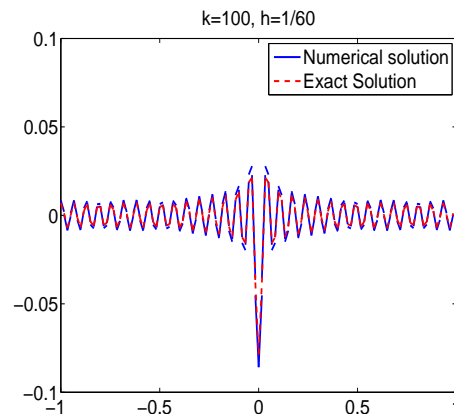


FIG. 4.11. *The trace plot along x -axis or $y = 0$ from WG solution using piecewise linear elements.*

REFERENCES

- [1] M. AINSWORTH, *Discrete dispersion relation for hp-version finite element approximation at high wave number*, SIAM J. Numer. Anal., 42, pp. 553-575, 2004.
- [2] M. AINSWORTH, P. MONK, AND W. MUNIZ, *Dispersive and dissipative properties of discontinuous Galerkin finite element methods for the second-order wave equation*, J. Sci. Comput, 27, pp. 5-40, 2006.
- [3] M. AINSWORTH AND H.A. WAJID, *Dispersive and dissipative behavior of the spectral element method*, SIAM J. Numer. Anal., 47, pp. 3910-3937, 2009.
- [4] D. N. ARNOLD, *An interior penalty finite element method with discontinuous elements*, SIAM J. Numer. Anal., 19(4), pp. 742-760, 1982.
- [5] D. N. ARNOLD AND F. BREZZI, *Mixed and nonconforming finite element methods: implementation, postprocessing and error estimates*, RAIRO Modl. Math. Anal. Numr., 19(1), pp. 7-32, 1985.
- [6] D. ARNOLD, F. BREZZI, B. COCKBURN, AND L. D. MARINI, *Unified analysis of discontinuous Galerkin methods for elliptic problems*, SIAM J. Numer. Anal., 39 (2002), pp. 1749-1779.
- [7] I. BABUŠKA, *The finite element method with Lagrange multipliers*, Numer. Math., 20 (1973), pp. 179-192.
- [8] I. Babuška, F. Ihlenburg, E.T. Paik, S.A. Sauter, A generalized finite element method for solving the Helmholtz equation in two dimensions with minimal pollution. *Computer Methods in Applied Mechanics and Engineering* 1995; **128**: 325-359.
- [9] I. Babuška, S.A. Sauter, Is the pollution effect of the FEM avoidable for the Helmholtz equation considering high wave number? *SIAM Journal on Numerical Analysis* 1997; **34**: 2392-2423. Reprinted in *SIAM Review* 2000; **42**: 451-484.
- [10] I. Babuška, U. Banerjee, and J. Osborn, *Generalized finite element method - main ideas, results, and perspective*, Internat. J. Comput. Methods, 1 (2004), pp. 67-103.
- [11] G. A. BAKER, *Finite element methods for elliptic equations using nonconforming elements*, Math. Comp., 31 (1977), pp. 45-59.
- [12] G. BAO, G.W. WEI, AND S. ZHAO, *Numerical solution of the Helmholtz equation with high wavenumbers*, Int. J. Numer. Meth. Engng, 59 (2004), pp. 389-408.
- [13] C. E. BAUMANN AND J.T. ODEN, *A discontinuous hp finite element method for convection-diffusion problems*, Comput. Methods Appl. Mech. Engrg., 175 (1999), pp. 311-341.
- [14] S. BRENNER AND R. SCOTT, *The Mathematical Theory of Finite Element Methods*, Springer-Verlag, New York, 1994.
- [15] F. BREZZI, *On the existence, uniqueness, and approximation of saddle point problems arising from Lagrange multipliers*, RAIRO, 8 (1974), pp. 129-151.
- [16] F. BREZZI AND M. FORTIN, *Mixed and Hybrid Finite Elements*, Springer-Verlag, New York, 1991.
- [17] F. BREZZI, J. DOUGLAS, JR., R. DURAN AND M. FORTIN, *Mixed finite elements for second order elliptic problems in three variables*, Numer. Math., 51 (1987), pp. 237-250.
- [18] F. BREZZI, J. DOUGLAS, JR., AND L.D. MARINI, *Two families of mixed finite elements for second order elliptic problems*, Numer. Math., 47 (1985), pp. 217-235.
- [19] A. BUFFA AND P. MONK, *Error Estimates for the ultra weak variational formulation of the Helmholtz equation*, ESAIM: Mathematical Modelling and Numerical Analysis, 42 (2008), pp. 925-940.
- [20] P. CASTILLO, B. COCKBURN, I. PERUGIA, AND D. SCHOTZAU, *An a priori error analysis of the local discontinuous Galerkin method for elliptic problems*, SIAM J. Numer. Anal., 38 (2000), pp. 1676-1706.
- [21] O. CESSENAT AND B. DESPRES, *Application of the ultra-weak variational formulation of elliptic PDEs to the 2-dimensional Helmholtz problem*, SIAM J. Numer. Anal., 35 (1998), pp. 255-299.
- [22] O. CESSENAT AND B. DESPRES, *Using plane waves as base functions for solving time harmonic equations with the ultra weak variational formulation*, J. Comput. Acoustics, 11 (2003), pp. 227-238.
- [23] S.N. CHANDLER-WILDE AND S. LANGDON, *A Galerkin boundary element method for high frequency scattering by convex polygons*, SIAM J. Numer. Anal., 45 (2007), pp. 610-640.
- [24] Z. CHEN, N.A. BAKER, AND G.W. WEI, *Differential geometry based solvation model I: Eulerian formulation*, J. Comput. Phys., 229 (2010), pp. 8231-8258.
- [25] E.T. CHUNG AND B. ENGQUIST, *Optimal discontinuous Galerkin methods for wave propagation*, SIAM J. Numer. Anal., 44 (2006), pp. 2131-2158.
- [26] P.G. CIARLET, *The Finite Element Method for Elliptic Problems*, North-Holland, New York, 1978.

- [27] B. COCKBURN AND C.-W. SHU, *The local discontinuous Galerkin method for time-dependent convection-diffusion systems*, SIAM J. Numer. Anal., 35 (1998), pp. 2440-2463.
- [28] B. COCKBURN AND C.-W. SHU, *Runge-Kutta Discontinuous Galerkin methods for convection-dominated problems*, Journal of Scientific Computing, 16 (2001), pp. 173-261.
- [29] B. COCKBURN, B. DONG, AND J. GUZMAN, *A superconvergent LDG-hybridizable Galerkin method for second-order elliptic problems*, Math. Comput. 77 (2008), pp. 1887-1916.
- [30] B. COCKBURN, J. GOPALAKRISHNAN, AND R. LAZAROV, *Unified hybridization of discontinuous Galerkin, mixed and continuous Galerkin methods for second-order elliptic problems*, SIAM J. Numer. Anal. 47 (2009), pp. 1319-1365.
- [31] C. HARHAT, I. HARARI, AND U. HETMANIUK, *A discontinuous Galerkin method with Lagrange multipliers for the solution of Helmholtz problems in the mid-frequency regime*, Comput. Methods Appl. Mech. Engrg., 192 (2003), pp. 1389-1419.
- [32] C. HARHAT, R. TEZAUER, AND P. WEIDEMANN-GOIRAN, *Higher-order extensions of a discontinuous Galerkin method for mid-frequency Helmholtz problems*, Int. J. Numer. Meth. Engrg, 61 (2004), pp. 1938-1956.
- [33] X. FENG AND H. WU, *Discontinuous Galerkin methods for the Helmholtz equation with large wave number*, SIAM J. Numer. Anal., 47 (2009), pp. 2872-2896.
- [34] B. X. FRAEIJLS DE VEUBEKE, *Displacement and equilibrium models in the finite element method*, In "Stress Analysis", O. C. Zienkiewicz and G. Holister (eds.), John Wiley, New York, 1965.
- [35] B. X. FRAEIJLS DE VEUBEKE, *Stress function approach*, International Congress on the Finite Element Methods in Structural Mechanics, Bournemouth, 1975.
- [36] E. GILADI, *Asymptotically derived boundary elements for the Helmholtz equation in high frequencies*, J. Comput. Appl. Math. 2007; **198**, 52-74.
- [37] R. GRIESMAIER AND P. MONK, *Error analysis for a hybridizable discontinuous Galerkin method for the Helmholtz equation*, J. Sci. Comput. 2011; in press.
- [38] I. Harari, T.J.R. Hughes, *Finite element methods for the Helmholtz equation in an exterior domain: model problems*, *Computer Methods in Applied Mechanics and Engineering* 1991; **87**: 59-96.
- [39] E. Heikkola, S. Monkola, A. Pennanen, and T. Rossi, *Controllability method for the Helmholtz equation with higher-order discretizations*. *J. Comput. Phys.* 2007; **225**: 1553-1576.
- [40] F. Ihlenburg, I. Babuška, *Dispersion analysis and error estimation of Galerkin finite element methods for the Helmholtz equation*. *International Journal for Numerical Methods in Engineering* 1995; **38**: 3745-3774.
- [41] F. Ihlenburg, I. Babuška, *Finite element solution of the Helmholtz equation with high wavenumber Part I: the h -version of the FEM*. *Computer and Mathematics with applications* 1995; **30**: 9-37.
- [42] F. Ihlenburg, I. Babuška, *Finite element solution of the Helmholtz equation with high wavenumber Part II: the h - p -version of the FEM*. *SIAM Journal of Numerical Analysis* 1997; **34**: 315-358.
- [43] Y. JEON, AND E. PARK, *A Hybrid Discontinuous Galerkin Method for Elliptic Problems*, SIAM J. Numer. Anal. 48 (2010), pp. 1968-1983.
- [44] S. LANGDON AND S.N. CHANDLER-WILDE, *A wavenumber independent boundary element method for an acoustic scattering problem*, SIAM J. Numer. Anal., 43 (2006), pp. 2450-2477.
- [45] J.M. MELENK AND I. BABUŠKA, *The partition of unity finite element method: Basic theory and applications*, Comput. Methods Appl. Mech. Engrg. 139, (1996), pp. 289-314.
- [46] P. MONK AND D.Q. WANG, *A least-squares method for the Helmholtz equation*, Comput. Methods Appl. Mech. Engrg. 175, (1999), pp. 121-136.
- [47] P. RAVIART AND J. THOMAS, *A mixed finite element method for second order elliptic problems*, Mathematical Aspects of the Finite Element Method, I. Galligani, E. Magenes, eds., Lectures Notes in Math. 606, Springer-Verlag, New York, 1977.
- [48] B. RIVIERE, M. F. WHEELER, AND V. GIRAULT, *A priori error estimates for finite element methods based on discontinuous approximation spaces for elliptic problems*, SIAM J. Numer. Anal., 39 (2001), pp. 902-931.
- [49] B. RIVIERE, M. F. WHEELER, AND V. GIRAULT, *Improved Energy Estimates for Interior Penalty, Constrained and Discontinuous Galerkin Methods for Elliptic Problems. Part I*, Computational Geosciences, volume 8 (1999), pp. 337-360.
- [50] A. H. SCHATZ, *An observation concerning Ritz-Galerkin methods with indefinite bilinear forms*, Math. Comp., 28 (1974), pp. 959-962.
- [51] Z.H. SHAO, G.W. WEI AND S. ZHAO, *DSC time-domain solution of Maxwell's equations*, J. Comput. Phys., 189 (2003), pp. 427-453.
- [52] J. SHEN AND L.-L. WANG, *Spectral approximation of the Helmholtz equation with high wave*

- numbers, SIAM J. Numer. Anal., 43 (2005), pp. 623-644.
- [53] J. SHEN AND L.-L. WANG, *Analysis of a spectral-Galerkin approximation to the Helmholtz equation in exterior domains*, SIAM J. Numer. Anal., 45 (2007), pp. 1954-1978.
 - [54] J. Wang and X. Ye, *A weak Galerkin finite element method for second-order elliptic problems*, Preprint submitted to SINUM, 2011.
 - [55] J. WANG, *Mixed finite element methods*, Numerical Methods in Scientific and Engineering Computing, Eds: W. Cai, Z. Shi, C-W. Shu, and J. Xu, Academic Press.
 - [56] S. ZHAO, *High order matched interface and boundary methods for the Helmholtz equation in media with arbitrarily curved interfaces*, J. Comput. Phys., 229 (2010), pp. 3155-3170.
 - [57] S. ZHAO, *Pseudo-time coupled nonlinear models for biomolecular surface representation and solvation analysis*, Int. J. Numer. Methods Biomedical Engrg., (2011), in press.
 - [58] O.C. Zienkiewicz, *Achievements and some unsolved problems of the finite element method*. *International Journal for Numerical Methods in Engineering* 2000; **47**: 9-28.